A systematic approach to testing and predicting light-material interactions

Zhang, Fan; de Ridder, Huib; Barla, Pascal; Pont, Sylvia C.

DOI
10.1167/19.4.11

Publication date
2019

Document Version
Final published version

Published in
Journal of vision

A systematic approach to testing and predicting light-material interactions

Fan Zhang Perceptual Intelligence Lab, Faculty of Industrial Design Engineering, Delft University of Technology, Delft, The Netherlands

Huib de Ridder Perceptual Intelligence Lab, Faculty of Industrial Design Engineering, Delft University of Technology, Delft, The Netherlands

Pascal Barla INRIA, University of Bordeaux, Talence, France

Sylvia Pont Perceptual Intelligence Lab, Faculty of Industrial Design Engineering, Delft University of Technology, Delft, The Netherlands

Photographers and lighting designers set up lighting environments that best depict objects and human figures to convey key aspects of the visual appearance of various materials, following rules drawn from experience. Understanding which lighting environment is best adapted to convey which key aspects of materials is an important question in the field of human vision. The endless range of natural materials and lighting environments poses a major problem in this respect. Here we present a systematic approach to make this problem tractable for lighting–material interactions, using optics-based models composed of canonical lighting and material modes. In two psychophysical experiments, different groups of inexperienced observers judged the material qualities of the objects depicted in the stimulus images. In the first experiment, we took photographs of real objects as stimuli under canonical lightings. In a second experiment, we selected three generic natural lighting environments on the basis of their predicted lighting effects and made computer renderings of the objects. The selected natural lighting environments have characteristics similar to the canonical lightings, as computed using a spherical harmonic analysis. Results from the two experiments correlate strongly, showing (a) how canonical material and lighting modes associate with perceived material qualities; and (b) which lighting is best adapted to evoke perceived material qualities, such as softness, smoothness, and glossiness. Our results demonstrate that a system of canonical modes spanning the natural range of lighting and materials provides a good basis to study lighting–material interactions in their full natural ecology.

Introduction

Lighting is a vital part of several artistic and industrial activities including photography, cinematography, theater, architecture, and design. Taking the example of photography, there are several common practices in setting up lighting environments that permit clear depiction of certain aspects of the shape or material of an object or subject. This is testified by the ever-growing list of tutorials found online, as well as in dedicated books on the topic (Hunter, Biver, & Fuqua, 2015). For example, key light sources may be employed to create highlights or body shadows, bringing out aspects such as glossiness and body shape, and fill lights are used to reduce shad(ow)ing, bringing out colors and delineating shape contours. Material appearance can be modulated by a judicious use of lighting tools; for example using hard-edged spot lights or so-called soft boxes at frontal, oblique, or grazing angles, and using white reflectors and/or black screens. As shown in Figure 1, lighting can render certain material qualities visible or invisible. The lighting techniques that permit to achieve such visual effects are usually learned from experience, with specific mechanisms applying to specific cases. The tutorials and books on this topic describe such specific cases, but lack a generic system to

Citation: Zhang, F., de Ridder, H., Barla, P., & Pont, S. (2019). A systematic approach to testing and predicting light-material interactions. *Journal of Vision*, *19*(4):11, 1–22, https://doi.org/10.1167/19.4.11.

https://doi.org/10.1167/19.4.11 Received June 14, 2018; published April 5, 2019 ISSN 1534-7362

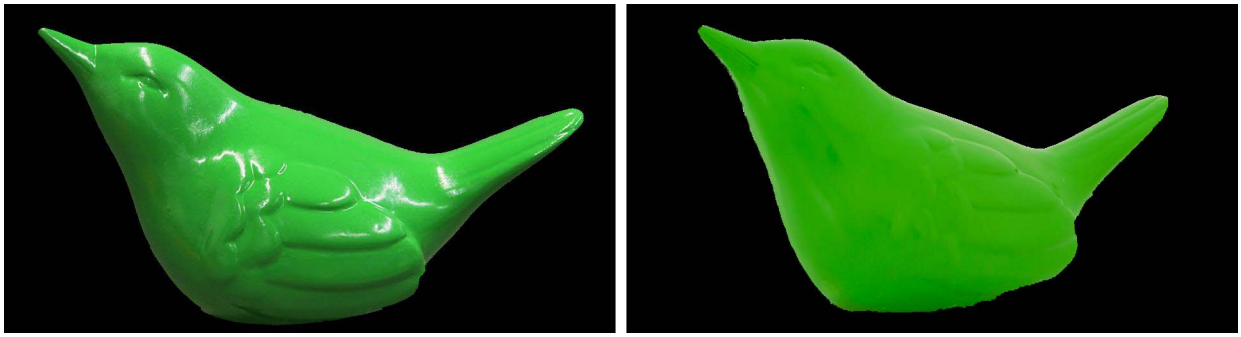

Figure 1. Photos of the same glossy bird-shaped object under two different illuminations. Left: a common office lighting environment; Right: a canonical ambient lighting environment. The object appears to be relatively smoother, harder, and glossier on the left.

predict lighting–material interactions for any material. Here we propose and test an approach to develop such a system.

An important goal in the field of human vision is to understand how lighting may affect appearance in generic scenes. In this paper, the specific aim is to understand and predict how lighting systematically influences material perception. We restrict our study to opaque materials and neglect texture. In the material perception literature, perceptual interactions between materials and lightings were previously reported by several studies, especially for matte versus glossy materials. For example, smooth surfaces appear glossier under collimated light sources than under broad diffuse light sources (Dror, Willsky, & Adelson, 2004; Pont & te Pas, 2006); different natural lighting environments have been shown to affect perceived glossiness to different amounts (Fleming, Dror, & Adelson, 2003; Döerschner, Boyaci, & Maloney, 2010; Olkkonen & Brainard, 2010; Marlow, Kim, & Anderson, 2012). More recently, Motoyoshi and Matoba (2012) found that changes in the contrast and gamma of the illumination affect perceived glossiness, and the orientation of highlights and the shape of highlights (due to differently shaped light sources) was found to affect the perception of gloss (Marlow, Kim, & Anderson, 2011; van Assen, Wijntjes, & Pont, 2016). Human judgments of qualities such as glossy, smooth, or soft have been found to be systematically related to material classes (Fleming, Wiebel, & Gegenfurtner, 2013) and lighting (Barati, Karana, Sekulovski, & Pont, 2017).

The main goal of this paper is to systematically study and predict the effects of a large variety of lighting environments on the perception of several qualities for a large range of materials. However, the range of naturally occurring lighting environments and materials seems to be endless, even if we restrict ourselves to opaque materials and neglect texture. In order to make this problem tractable, we propose an approach on the basis of canonical modes; that is, stereotypical representations of the basic components of naturally occurring light and materials. Here we use three lighting and four material modes, following our previous work on the topic (Zhang, de Ridder, & Pont, 2015; Barati et al., 2017). The modes are based on an optical model describing natural light fields (Mury, Pont, & Koenderink, 2007) and several optical models describing the bidirectional reflectance distribution functions (BRDFs) of opaque materials (Ward, 1992; Koenderink & Pont, 2003; Barati et al., 2017). The modes can occur in isolation but can also be linearly superposed in order to create generic luminous environments and materials, analogous to how semi-glossy materials can be rendered using linear combinations of matte and specular reflectance components. Specifically, for the lighting we consider an *ambient light mode* consisting of a spherically diffuse light environment, a *focus light mode* represented by a collimated light source, and a *brilliance light mode* in the form of a large number of small light sources. These modes represent the zero order, first order, and higher order contributions of a spherical harmonic decomposition of the local light field (Mury, Pont, & Koenderink, 2007), have a physical and perceptual meaning (Pont, 2009), and correspond to the basic layers that are used in perception-based lighting design (Kelly, 1952; Ganslandt & Hofmann, 1992; Pont, 2009). For the materials, we covered smooth objects with four different types of finishes: matte paint, glossy paint, a velvet-like (or flocked) layer, and a glittery layer, representing, respectively, a constant BRDF (diffuse scattering), a peaked BRDF in the forward (mirror) direction, a BRDF that "explodes" along the surface (asperity scattering), and a broadened noisy BRDF (specular multifacet scattering). We denote these material modes by the terms *matte*, *specular*, *velvety*, and *glittery*, respectively.

The hypothesis we want to test is whether some characteristics of lighting are more amenable to convey material qualities than others, and if yes, which ones? In one of our previous studies (Zhang et al., 2015), we found that the brilliance lighting could make certain material appear glossier but less velvety than the focus

lighting. In our former research, we also found that for the modes we used, the matching and comparison results were more robust for materials than for lighting. In that study, we did not test which qualities were perceived for our lighting–material combinations. So the first goal of the current study is to test a large range of material qualities and how they are brought out by specific lighting–material combinations. We take on a systematic approach, both with real and synthetic stimuli, to determine whether our canonical modes can help understand and predict the effects.

In Experiment 1, we test how our stimuli map onto the space of perceived material qualities. To this end, we conducted a rating task using real stimuli photographed under three canonical lighting modes. In order to test whether these observations remain valid for natural lighting environments, we conducted Experiment 2 to model and validate the canonical approach. First, we have quantitatively analyzed environment maps (Debevec, 1998) from the University of Southern California (USC) database (http://gl.ict.usc.edu/Data/HighResProbes/; accessed October 23, 2015) and selected three candidate lightings that best represent the canonical ones. The selection was done on the basis of the power of the components of their spherical harmonic decompositions. The canonical material modes were similar to the ones used in an earlier study in which we compared real to rendered materials (Zhang, de Ridder, Fleming, & Pont, 2016). We then rendered objects of the four canonical material reflectance modes in the three selected lighting environments that best approach the canonical lighting modes. In Experiment 2 we then conducted the same rating experiment as in Experiment 1 using rendered stimuli and selected natural lighting environment maps. The main motivation to conduct Experiment 2 was to model and simulate the canonical modes, and see if we could validate the canonical approach for generic illumination environments. This is interesting for both perception and computer graphics studies. After all, it is easier to render stimuli than photograph real materials under controlled lighting environments. First, we repeated the analysis of Experiment 1 for Experiment 2 to test how the combinations of modes map onto the data space of perceived material qualities. Next, we tested our predictions that the selected generic natural lighting environments would have similar effects depending on the material mode, as in Experiment 1, via detailed comparisons of the results between the two experiments. These detailed comparisons reveal strong correlations, confirming that lighting–material effects are systematic and can be predicted based on a coarse categorization into canonical modes. In the discussion, we address limitations and future challenges of this systematic approach.

Method

Real stimuli: Experiment 1

In Experiment 1, the stimuli were the cropped images processed from the photos taken from multiple copies of the same real bird object under three canonical lighting modes. The objects were covered with matte, velvety, specular, and glittery finishes to represent the four canonical material modes (Figure 2). For the ambient light, we put both the birds and the camera in a white photo tent and illuminated the photo tent with fluorescent tube lamps from the ceiling. For the focus light, we illuminated the birds with a halogen lamp from upper left. For the brilliance light, we surrounded the birds with 150 LED lights. The same images were previously used as stimuli in a matching experiment (Zhang et al., 2015) to study the lighting–material interactions. All photographs were taken using a Canon EOS 400D DIGITAL camera (focal length 57 mm) in controlled laboratory environments, then edited to find the shared contour and make the background black (resolution 954×512 pixels). The luminance was photometrically calibrated to be linear.

Rendered stimuli: Experiment 2

Illumination environments

In order to validate our canonical modes approach, we extended it to generic natural lighting environments and tested whether this allows for coarse predictions of the lighting effects on material appearance. Thus, we took a small database of natural illumination maps and then aimed to recreate the effects of Experiment 1. From the USC's high resolution recreations of the Debevec's light probe images we selected three maps that optically should be the best representatives of the ambient light, focus light, and brilliance light in this database. First, we reconstructed the spherical function of the illumination environment $f(\theta, \phi)$ by the sum of its spherical harmonics (SH):

$$f(\theta,\phi) = \sum_{l=0}^{\infty} \sum_{m=-l}^{l} C_l^m \cdot Y_l^m(\theta,\phi), \quad (1)$$

where C_l^m are the coefficients, $Y_l^m(\theta, \phi)$ are the basis functions, and l is the order of the angular mode varying from zero to infinity. The power of the l-th order, denoted as d_l, physically characterizes the angular distributions of the illumination at order l, which is orientation-invariant and can be calculated as (Stock & Siegel, 1996):

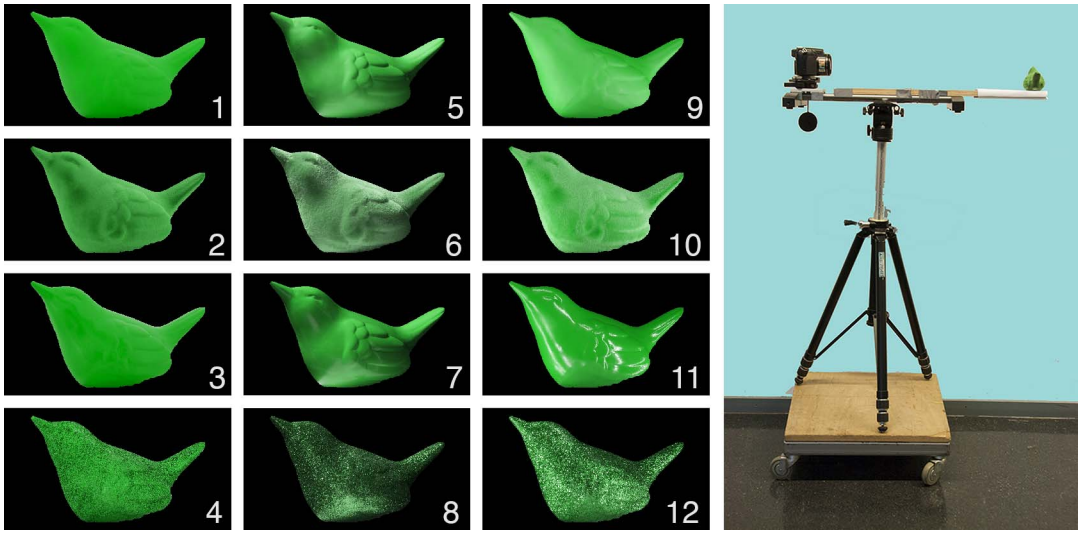

Figure 2. Left: The stimuli of Experiment 1. From top to bottom, the four rows represent the matte, velvety, specular, and glittery material modes. From left to right, the three columns represent the ambient, focus, and brilliance lighting modes. Right: the photography setup, which kept the relative position of the object and the camera fixed when switching (riding) between lighting environments. All photographs were taken (using a Canon EOS 400D DIGITAL camera, focal length 57 mm) in controlled laboratory environments, edited to find the shared contour and make the background black (resolution 954×512). The luminance was photometrically calibrated to be linear.

$$d_l = \sqrt{\sum_{m=-l}^{l} \left(C_l^m\right)^2}. \quad (2)$$

Using Xia's diffuseness metric (Xia, Pont, & Heynderickx, 2017) we could calculate the diffuseness of all high-resolution high dynamic range (HDR) maps, via the ratio of the power of the first order $d_{l=1}$ to the power of the zeroth order $d_{l=0}$ of the SH decomposition. By normalization, diffuseness scores range between 0 (zero), which corresponds to extremely directed lighting (i.e., focus lighting) to 1, which corresponds to fully diffuse lighting (i.e., ambient lighting), as in the equation below:

$$(D_{xia})_{Normalized} = 1 - d_{l=1}/d_{l=0}/\sqrt{3}. \quad (3)$$

As a result, the *Glacier* environment map scored the highest in Xia's diffuseness metric and was being selected as the representative map for the ambient light; the *Ennis* environment map scored the lowest in Xia's diffuseness metric and thus, was selected as the representative map for the focus light (Figure 3, on the left).

To select the Debevec environment map that could best represent the brilliance lighting mode, we propose a brilliance metric, calculating the ratio between the sum of the higher orders statistics ($l \geq 3$) to the sum of all orders:

$$B = \frac{\sum_{l=3}^{\infty} d_l}{\sum_{l=0}^{\infty} d_l}. \quad (4)$$

The result of the brilliance metric B will vary from 0 (no brilliance at all) to 1 (pure brilliance). In practice, we implemented finite sampling and found that the brilliance metric gave robust results beyond the 10th order. As shown in Figure 3, the *Grace-new* lighting scored the highest in our brilliance metric when calculating up to the 10th order or higher, and thus was selected as the representative map for the brilliance lighting. The selected maps can be seen in the top row of Figure 4.

The illumination environments are provided as HDR panoramic images. Since their main lighting directions occur in different locations than our canonical focus lighting, we had to manually adjust their orientations such that their light directions in the first order spherical harmonics were matched. They were adjusted per type of lighting by applying a rotation of θ radians around the horizontal camera axis, followed by a rotation of ϕ radians around the vertical camera axis. In particular, the brilliance lighting had to be rotated around the horizontal camera axis. For the values, see Table 1. Each illumination environment was then converted from RGB to gray values (i.e., the relative luminance) using the formula: $0.2126 \times R + 0.7152 \times G + 0.0722 \times B$ (Stokes, Anderson, Chandrasekar, & Motta, 2012).

Material modes

We considered four different material modes: matte, glossy, glittery, and velvety. Each mode may be

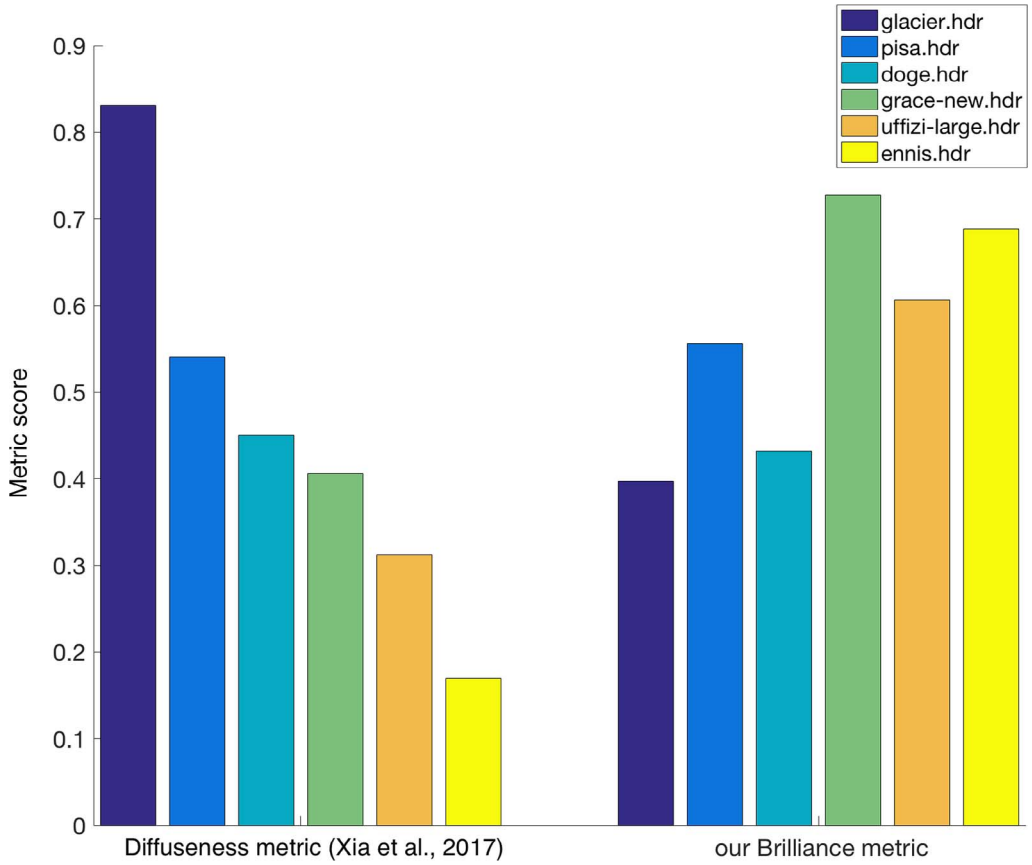

Figure 3. Metrics using the spherical harmonics decomposition for the USC high-resolution HDR maps. Left: results of the diffuseness metric (Xia et al., 2017) used to select the Glacier map for the ambient lighting and the Ennis map for the focus lighting. Right: results of the brilliance metric sampled up to the 10th order.

described by its BRDF $f_r(\omega_i, \omega_o)$, where ω_i represents an incoming direction vector (e.g., from a light source) and ω_o represents an outgoing direction vector (e.g., toward the viewpoint). Note that both vectors ω_i and ω_o are defined by two angles. In computer graphics, f_r outputs three values, one for each of the RGB color channels. Table 2 provides the parameters used in these BRDFs. They are explained in the following list:

a. The *matte material mode* was implemented with a Lambertian BRDF; that is,

$$f_r(\omega_i, \omega_o) = \frac{\rho_d C_d}{\pi} \quad (5)$$

where $\rho_d \in [0, 1]$ controls the intensity of the Lambertian reflectance, and C_d is a color that we set to {24, 253, 22} in RGB to yield a greenish tint resembling the stimuli of Experiment 1. All other material modes exhibit a diffuse component with the *same* color, but a potentially *different* intensity as detailed in Table 2.

b. For the *velvety material mode*, we used the asperity scattering BRDF model of Koenderink and Pont (2003), to which we also added a diffuse term as before, yielding:

$$f_r(\omega_i, \omega_o) = \frac{\rho_d C_d}{\pi} + \frac{\rho_v}{2 \cos\theta_i \cos\theta_o} \quad (6)$$

where ρ_v controls the intensity of the velvety component. This model assumes asperity scattering to be isotropic.

c. The *specular material mode* was implemented with an isotropic Ward BRDF (Ward, 1992):

$$f_r(\omega_i, \omega_o) = \frac{\rho_d C_d}{\pi} + \frac{\rho_s}{4\pi\alpha_s^2\sqrt{\cos\theta_i \cos\theta_o}} e^{-\frac{\tan^2\theta_h}{\alpha_s^2}} \quad (7)$$

where θ_i, θ_o, and θ_h denote angles made by either ω_i, ω_o or $h = \frac{\omega_i + \omega_o}{\omega_i + \omega_o}$ with the surface normal. The $\rho_s \in [0, 1]$ parameter controls the intensity of the glossy reflection, while $\alpha_s \in [0, 1]$ controls the roughness of the material (higher values meaning blurrier reflections).

d. The *glittery material mode*: we simulated the broadened and noisy forward scattering of the glittery material by mimicking the occurrence of multifacet flakes at the surface of the object. The

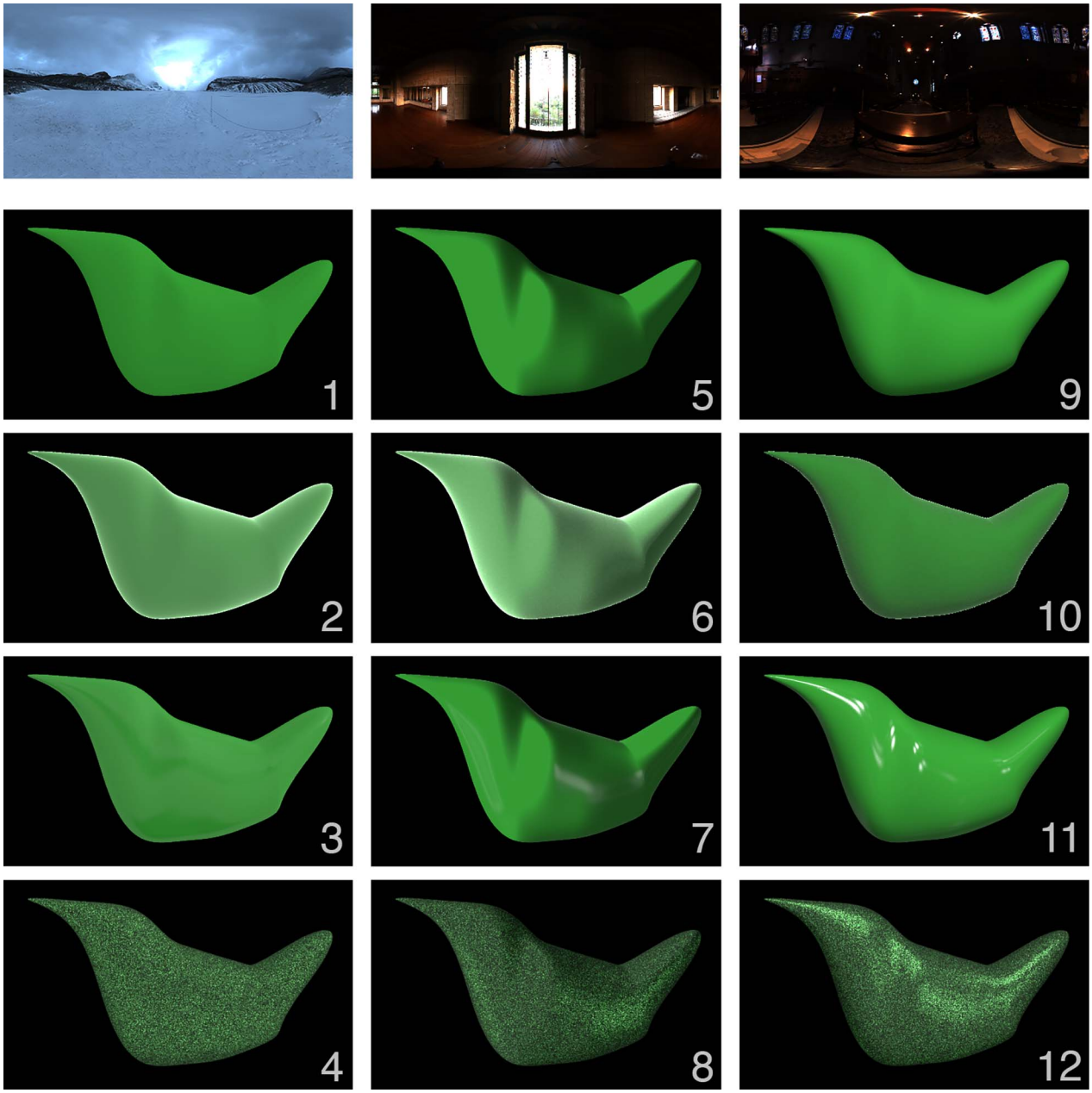

Figure 4. The stimuli of Experiment 2. From top to bottom, the first row shows the three lighting maps we selected to be the best representatives for the canonical lighting modes of the high resolution USC database. The second to the last rows represent the rendered matte, velvety, specular, and glittery material modes. From left to right, the three columns represent the materials under the Glacier, the Ennis, and the Grace-new illumination environments, respectively, as visualized in the first row. Compared to the initial Glacier environment, our version has been modified by filling in the black region originally found at the bottom of the image (which is due to the tripod base). The gammas of the images for the glittery mode (last row) were adjusted from 1.0 to 1.8 in order to make the features more visible in the printed version.

	θ	ϕ
L1: Glacier (ambient)	−0.170	−1.796
L2: Ennis (focus)	−0.170	1.413
L3: Grace-new (brilliance)	−0.961	−0.615

Table 1. The orientation parameters per illumination environment.

Mode	Parameters		
Matte	$\rho_d = 0.687$		
Velvety	$\rho_d = 0.4$	$\rho_v = 0.4$	
Specular	$\rho_d = 0.687$	$P_s = 0.067$	$\alpha_s = 0.037$
Glittery	$\rho_d = 0.5$	$P_s = 0.9$*	$\alpha_s = 0.1$

Table 2. Parameters used in each mode. The * symbol indicates a surface-varying parameter.

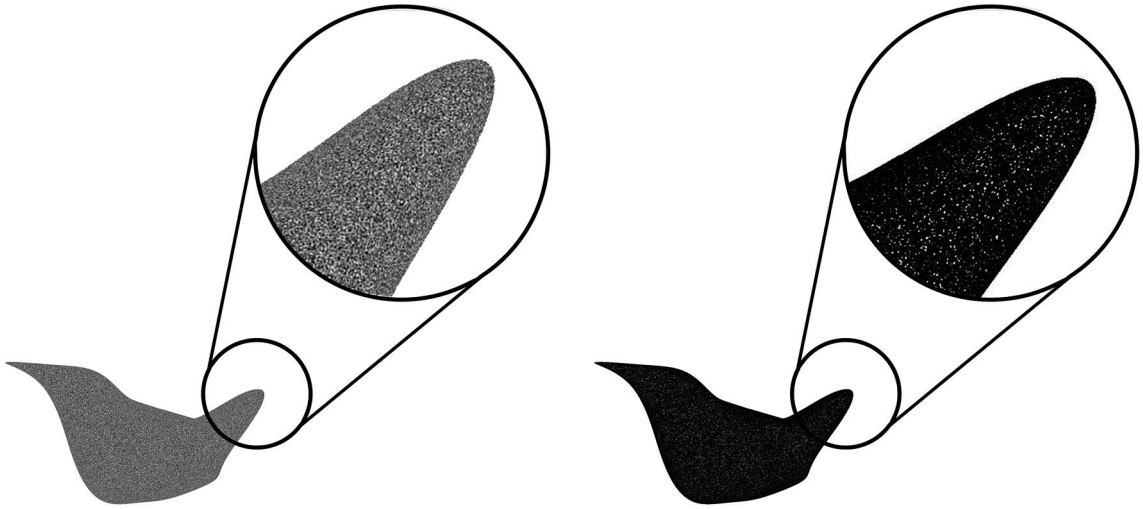

Figure 5. The sparsity of the distribution of the flakes for glittery effects, with zoomed view for the tails. Left: output of the Gabor noise function *N*. Right: remapping of *N* values to yield a sparser distribution of apparent flakes.

first step in our mimicking procedure was to use the BRDF of the specular material mode, varying the ρ_s parameter. To this end, we used an isotropic Gabor noise (Lagae, Lefebvre, Drettakis, & Dutré, 2009), which permits the production of an even distribution of flakes as shown in the left part of Figure 5. We employed the implementation of Lagae and Drettakis (2011), using a tangent space distribution of 150 impulses with frequency of 0.157, bandwidth of 2.724, and truncated to 0.013. The sparsity of the distribution was then adjusted by remapping noise values N to $r_s = 0.9 \times \left|(1.1 \times smoothstep(0, 1, N))^8\right|_0^1$, where $|\cdot|_0^1$ clamps values between 0 and 1; this is shown in the right part of Figure 5. Exponentiation permits selection of the brightest noise values, the 1.1 factor slightly saturates them to obtain apparent flakes of varying size, while the GLSL *smoothstep* function softens the selection.

The second step in the mimicking procedure was to additionally modify the surface normals by a different noise function to take into account the slight variations of flake orientations with respect to the object surface. This time we used a value noise based on the position of each surface point in 3D, with an amplitude of 1.0, a frequency of 0.157 (same as before), a persistence of 0.8, and four octaves. It is used to perturb the direction of the normal around the local geometric normal.

Rendering process

The 3D modeling of the bird shape was created in Blender (Blender 2.79b; Blender Foundation, Amsterdam, the Netherlands), as a simplified version of the shape of the real objects, and is the same as the 3D model we used in previous work (Zhang et al., 2016). The black region at the bottom of the Glacier environment map (due to the tripod base) was filled in to make it more ambient and natural (shown in Figure 4). The filled-in version of the Glacier environment map can be found in the supplementary materials (Supplementary Figure S1, Supplementary Figure S2, and Supplementary Figure S3). To render the stimuli of Experiment 2 we used Gratin version 0.3 for Apple Mac OS (Vergne & Barla, 2015) with rendering made using OpenGL shading language (GLSL) version 410.

Rendering was performed ignoring shadowing and interreflection effects. The diffuse component may then be equivalently represented using a diffuse-filtered version of the illumination environment, as provided on the USC website (diffuse convolution links). Rendering the diffuse component then simply amounts to look up the diffuse-filtered environment in the direction of the surface normal. We used this pre-filtered approach as it completely removes noise coming from the rendering process of the diffuse component. For the other components, we employed Monte Carlo integration, using importance sampling of the Ward material (i.e., for the specular and glittery modes) to speed up convergence. The rendering results (i.e., the stimuli for Experiment 2) can be found in Figure 4.

Procedure

The same procedure was used in both Experiments 1 and 2. For each observer, a list of nine qualities was first explained before the experiment started. The list consisted of the four names of our canonical material modes, namely matte, velvety, specular, and glittery;

and five terms that are often used in material perception studies, namely hard, soft, rough, smooth, and glossy (Fleming et al., 2013; Barati et al., 2017). All stimuli were then shown twice in random order to give the observers an idea about how different the stimuli are from each other, so that they could use the whole scale during the following rating procedure. In each trial, the observers had to answer two questions, the first one being a yes or no question: "Is the bird [. . .]?", with the [. . .] displaying one of the nine qualities?" If they answered Yes, they would then have to answer the second question, "how [. . .] is the bird on a scale from 1 to 7?" by moving the cursor on a slider. If they answered No to the first question, they would skip the second question and jump to the next trial. The observers were explicitly instructed that they did not have to balance the answers of the yes or no questions. With 12 stimuli, nine material quality terms, and three repetitions, there were 324 trials per observer per experiment. The trials were presented in nine blocks based on the qualities. The nine blocks were presented in a randomized order across observers. The interface was developed with the Psychophysics Toolbox extensions (Brainard, 1997; Kleiner et al., 2007) in MATLAB R2016b (MathWorks, Natic, MA), and presented on a linearly calibrated Apple Inc. 15-in. Retina display, with a resolution of 1440×900 pixels, ranging from 0.11 cd/m^2 to 75 cd/ m^2. The stimulus was presented as 954×512 pixels in the middle of the screen. The viewing distance between the observer and the screen was about 0.5 m and kept constant.

Observers

Fifteen paid observers participated in Experiment 1. A different group of 12 paid observers participated in Experiment 2. All participants had normal or corrected-to-normal vision, and were inexperienced in psychophysical experiments. Participants read and signed a consent form before the experiments were conducted. The study was approved by the Human Research Ethics Committee at Delft University of Technology, and conducted in accordance with the Declaration of Helsinki and Dutch law.

Analysis

To investigate how our canonical modes map onto the space of perceived material qualities, for both Experiment 1(real stimuli) and 2 (rendered stimuli) we analyzed the Yes or No (Y/N) data to see (a) whether the four names (matte, velvety, specular, and glittery) agree with the corresponding material modes, and (b) how combinations of canonical material and lighting

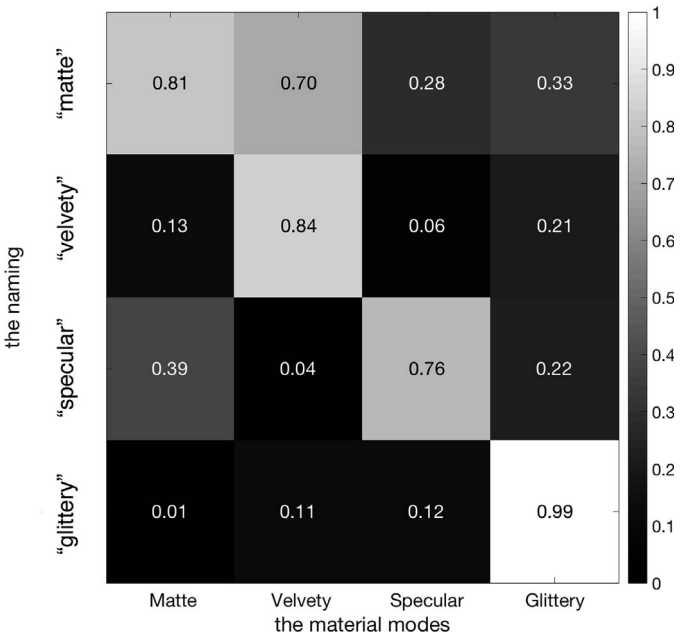

Figure 6. The fraction of answering Yes for the four material modes in Experiment 1.

modes associate with perceived qualities. To answer the first question, the raw data of the Y/N results for the four names are presented as percentage of answering Yes for each material mode. To answer the second question, we performed a correspondence analysis (CA) on the Y/N data for all qualities to further present the associations between the modes and qualities. Subsequently, we performed a principle component analysis (PCA) on the rating data to further explore the data space of perceived material qualities and how our real and rendered stimuli are positioned in that space. Finally, we compared the raw rating data and the PCA data space of Experiment 1 with those of Experiment 2 to examine how well the renderings correlate with the real objects, and to look into how lightings evoke material dependent effects for material modes.

Experiment 1

Analysis and results

Yes/No data

The first issue we wanted to look into was whether the names matte, velvety, specular, and glittery for the four canonical material modes agrees with the observers' judgments. To answer this, we analyzed the relevant subset of the results from the Y/N questions. In Figure 6, the percentage of answering Yes for each quality is shown per material mode (i.e., the fractions of responses for the names matte, velvety, specular, and

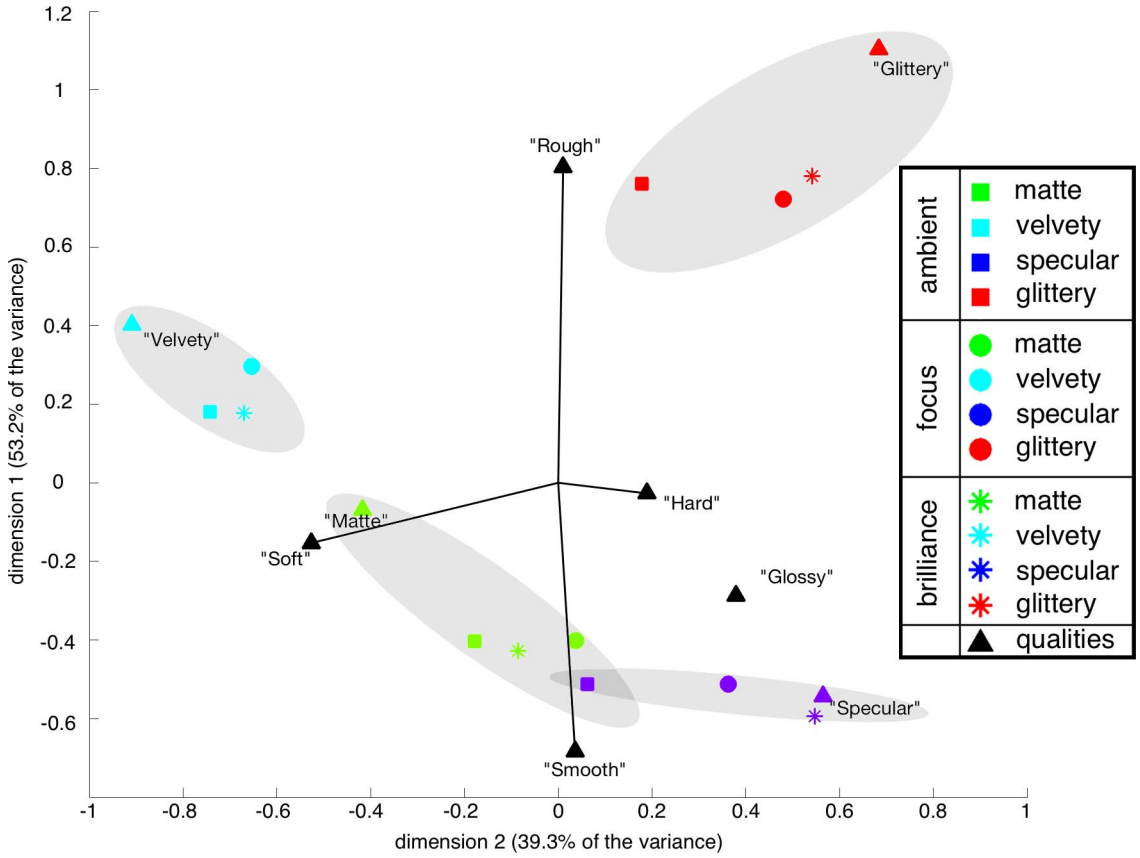

Figure 7. Visualization of the correspondence analysis results of the Y/N data for Experiment 1. The first dimension (*y*-axis) explains 53.2% of the variance. The second dimension (*x*-axis) explains 39.3% of the variance. The stimuli of the same material mode and their corresponding qualities are colored the same, specifically matte in green, velvety in light blue, specular in indigo, and glittery in red. The other five qualities are colored black. The same shape marks the stimuli of the same lighting mode, specifically ambient light as squares, focus light as circles, and brilliance light as stars. The triangles represent the nine qualities that were tested in the Y/N question. The gray ellipses were drawn by hand to show the material clusters. Please note that we connected the origin to soft, hard, rough, and smooth only to show that soft and hard as well as smooth and rough form opposing pairs of qualities and that these two opponent pairs were orthogonal to each other, in line with existing literature (e.g., Fleming et al., 2013). The same was done in Figure 10.

glittery) averaged across three lightings (for all Y/N data per lighting–material condition, see Figure S1), coded as a gray level. Each row represents a quality and each column represents a stimulus material mode. Note that for each row or column, the percentages of the four values do not necessarily add up to 100%. In general, the names were found to be associated with the material modes ($\chi^2(9) = 571, p < 0.01$). The diagonal values show the percentages of the answers for the congruent naming and material modes. It shows that the names velvety, specular, and glittery agree with the corresponding material modes, as those diagonal values are 0.84, 0.76, and 0.99, respectively. Although the name matte was found to agree with the observers' responses to our matte material (0.81), it also applied to our velvety material (0.70), and sometimes also to the specular (0.28) and glittery (0.33) modes. This mostly applied to the stimuli under the ambient light (0.58 for specular mode and 0.53 for glittery mode), sometimes to the stimuli under the focus light (0.27 for specular mode and 0.29 for glittery mode), and less often to the stimuli under the brilliance light (0.18 for the glittery mode and never for the specular mode). Meanwhile, the name specular also sometimes applied to the matte stimuli (0.39), mostly under the focus lighting (0.64), and sometimes to the ambient lighting (0.24) and the brilliance lighting (0.27). These results confirm our previous findings about the interactions between matte and specular material modes (Zhang et al., 2015; Zhang et al., 2016).

We further analyzed the results of the Y/N questions by performing a correspondence analysis (CA) using all nine qualities. In a 2D correspondence analysis biplot, we visualized the association between the labels based on their proximity (i.e., their distances in that space) and the distinctness based on their distances to the origin. The closer the data points are to each other, the better they associate. The resulting 2D CA biplot of the Y/N questions for Experiment 1 can be found in Figure 7. We observe that the name matte is relatively closer

to the origin than the other names (velvety, specular, and glittery). The stimuli of the specular and glittery material modes cluster closely around their corresponding names specular and glittery, respectively. Velvety stimuli cluster in the middle of the names matte and velvety, showing that both names could apply to the velvety material mode. Similarly, the matte stimuli cluster in the middle of the names matte and specular, in line with the finding that the name specular also sometimes applied to the matte stimuli (Figure 6). These observations suggest that the names velvety, specular, and glittery applied to the corresponding material modes, while for matte, there were larger variations. We also see that the lighting modes have greater influence on the judgments for the specular and glittery materials with brilliance lighting and ambient lighting having the largest and smallest impact, respectively. This effect is virtually absent for the matte and velvety materials. Lastly, note that the space has been rotated 90° anticlockwise and then mirrored around the vertical axis. The resulting *y*-axis, being the first dimension explaining 53.2% of the variance, shows *rough* and *smooth* as opposing qualities while the second dimension (*x*-axis), explaining 39.3% of the variance, shows *soft* and *hard* as opposing qualities. Figure 7 also shows that glittery material is primarily associated with rough, specular material with smooth and glossy, velvety material with soft, and matte material with smooth. Hard is close to the origin, meaning that it is associated with almost all stimuli except for velvety material.

Rating data

Here we analyze in depth whether certain types of material qualities are actually evoked by certain characteristics of the canonical lighting environments, and if so, to what extent. To answer this, we analyzed the results from the rating sessions by performing a PCA. Since the observers only had to give a rating when they answered Yes, we took all No answers as zero and together with the scale of 1 to 7, we took the medians across repetitions and observers to perform the PCA. The first three principle components (PCs) accounted for 97% of the data variance, with the first and second dimension explaining 52% and 34%, respectively. We therefore believe that a 2D PCA space suffices to visualize the apparent differences between our stimuli. Figure 8 shows the resulting data via a 2D PCA biplot, with the data being color-coded for the stimulus material; specifically matte in green, velvety in light blue, specular in indigo, and glittery in red. The four corresponding qualities are colored in corresponding colors and the other five qualities are colored in black. The shape marks the lighting mode, specifically ambient light as squares, focus light as circles, and brilliance light as stars. The qualities hard, specular, and glossy load positively on the first principle component PC1, while the qualities soft, matte, and velvety load negatively on PC1. Similarly, the qualities rough and glittery load positively on the second principle component (PC2), while the quality smooth loads negatively on this second component. Furthermore, projecting the stimuli data points onto the quality axes helps us understanding the lighting effects. Per material, the more the projected data points shift along the quality axes, the stronger the change of lighting affects the perception of that quality. For example, the specular stimuli data points (colored in indigo) shift away from the center along the axes of specular, glossy, smooth, and hard as the lighting varies from ambient (square) to focus (circle), and then to brilliance (star). This indicates that the brilliance lighting strongly evoked the quality specular, while ambient light weakened perceived specularity for our specular material mode, confirming earlier findings. Similarly, we found that the ambient light weakened the perception of glittery, hard, and rough for the glittery mode, while it evoked the perception of matte and soft for the matte mode. Other lighting effects were more subtle and will be discussed in detail in the Comparison section hereafter.

Experiment 2

Analysis and results

The analysis of the data of Experiment 2 was done analogous to and in the same order as that of Experiment 1; that is, we first looked into the Y/N data and then into the rating data.

Yes/No data

Figure 9 shows the averaged percentage of answering Yes for each material mode quality in the same format that was used in Figure 6. The averaging was again done across the three lightings (for all Y/N data per lighting–material condition, see Figure S2). Each row represents one quality and each column represents a stimulus material mode, so the diagonal values show the percentages of the answers for the correct naming of the corresponding material modes. Overall, the results are similar to the results of Experiment 1. The names were again found to be associated with the material modes ($\chi^2(9) = 589, p < 0.01$). The diagonal values are 0.87, 0.96, 0.76, and 1.00 for matte, velvety, specular, and glittery, respectively. There are two remarkable differences between the two experiments:

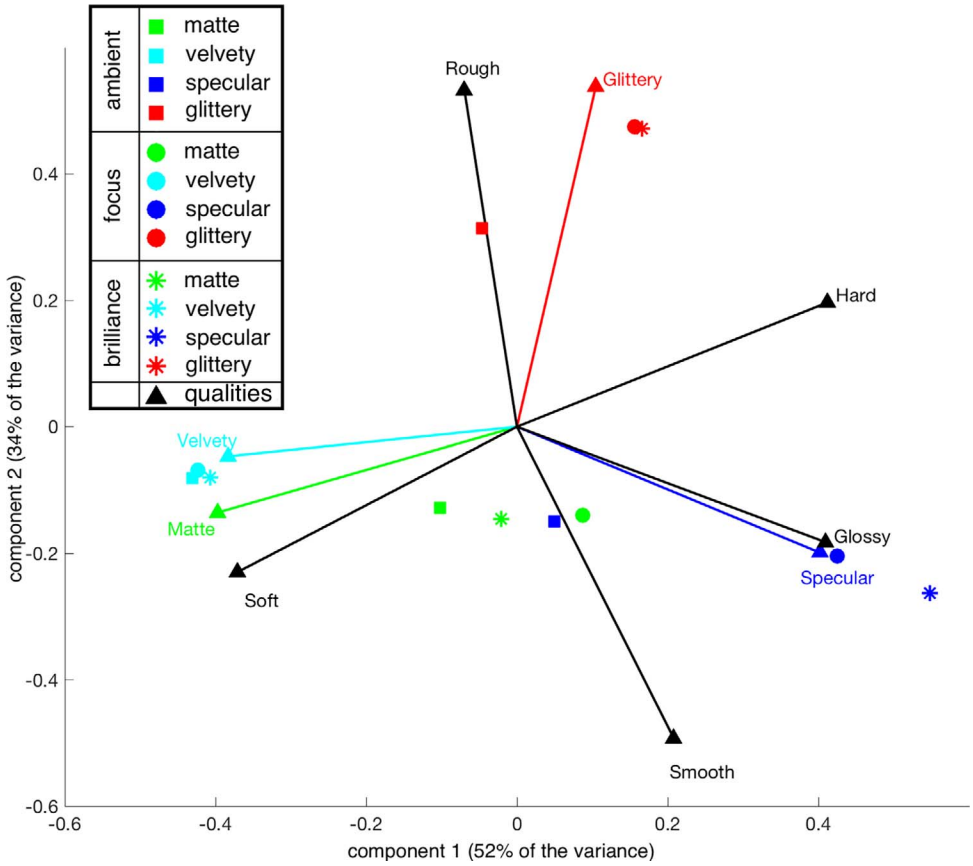

Figure 8. Results of the principle component analysis (PCA) for Experiment 1. The PCA was done on the ratings per material quality per stimulus, with the medians determined across all observers and repetitions. The first component (*x*-axis) explains 52% of the variance. The second component (*y*-axis) explains 34% of the variance. The stimulus materials and their corresponding qualities are color-coded, specifically matte in green, velvety in light blue, specular in indigo, and glittery in red. The other five qualities are colored black. The shapes mark the stimulus lighting, specifically ambient light as squares, focus light as circles, and brilliance light as stars.

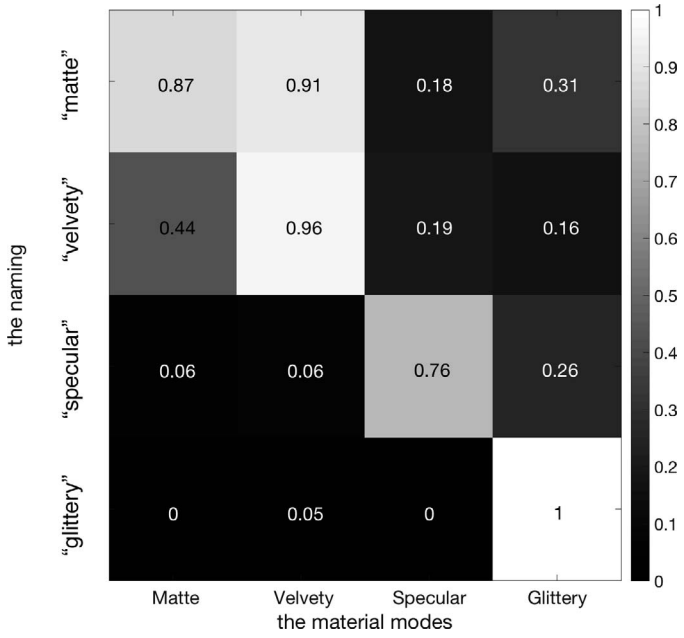

Figure 9. The fraction of answering Yes for the four material modes in Experiment 2.

first, the interaction between matte and velvety increased as the matte material was more often named velvety (0.44) and at the same time, the velvety material was more often named matte (0.91) compared to Experiment 1 (for which we found 0.13 and 0.70, respectively). This confirmed our previous findings about the increased interactions between matte and velvety materials when using computer rendered stimuli (Zhang et al., 2016). Second, the name specular was hardly used for the matte renderings (0.06), in contrast with the frequent naming in Experiment 1 (0.39).

The 2D correspondence analysis results are shown in the biplot in Figure 10. Although the lightings were generic natural lighting environments instead of laboratory conditions, we observe quite similar results as in Experiment 1. The first axis, which explains 53% of the variance, shows soft and hard again as opposing qualities. Similarly, the second axis, which explains 40.8% of the variance, shows rough and smooth, also as opposing qualities. Compared to the results from Experiment 1 (Figure 7), the only main difference is

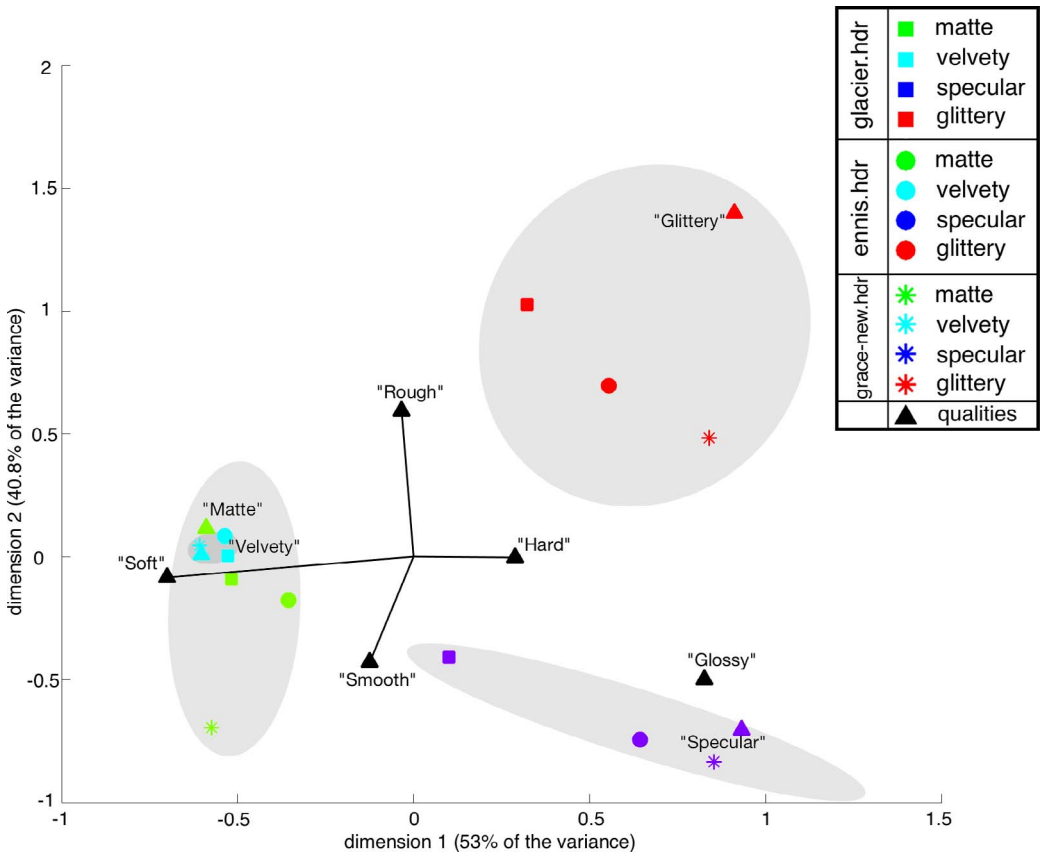

Figure 10. The visualization of the correspondence analysis results of the Y/N data for Experiment 2. The first dimension (*x*-axis) explains 53% of the variance. The second dimension (*y*-axis) explains 40.8% of the variance. The stimuli of the same material mode and their corresponding qualities are colored the same, specifically matte in green, velvety in light blue, specular in indigo, and glittery in red. The same shape marks the stimuli of the same lighting mode, specifically ambient light as squares, focus light as circles, and brilliance light as stars. The triangles represent the nine qualities that were tested in the Y/N question. The gray ellipses were intuitively drawn to show the distance between each stimulus and the quality. As in Figure 7, we connected the origin to soft, hard, rough, and smooth only to show that the two opponent pairs were orthogonal to each other.

that the clusters for matte and velvety shifted closer to each other, confirming the increased interactions between the matte and velvety modes.

Rating data

We also performed a PCA on the medians of the ratings for Experiment 2, in which the medians were calculated across repetitions and observers. The first three PCs accounted for 95% of the data variance, with the first and second components explaining 49% and 35%, respectively. The results are visualized as a 2D biplot in Figure 11. The legends are the same as in Experiment 1. Figure 11 indicates that, similar to Experiment 1, the qualities hard, specular, and glossy load positively on PC1, while the qualities soft, matte, and velvety load negatively on PC1. The qualities rough and glittery load positively on the PC2, while the qualities smooth, specular, and glossy load negatively on PC2. In line with the observation that the overall space created from the results of Experiment 2 is similar to that of Experiment 1, the specular stimuli again shift away from the center along the specular, glossy, smooth, and hard axes, when the lighting changed from Glacier environment (the most representative light map for the ambient light) to Ennis environment (the most representative light map for the focus light), and then to Grace-new environment (the most representative light map for the brilliance light). The same holds for the glittery stimuli shifting away along the hard axis. Matte and velvety stimuli data points clustered more closely to each other, indicating that they were affected more subtly as the lighting varied. More detailed material-dependent lighting effects will be discussed in the next section.

Comparison (real stimuli vs. renderings)

Here we compare the rating results from the two experiments. Figure 12 displays a direct comparison

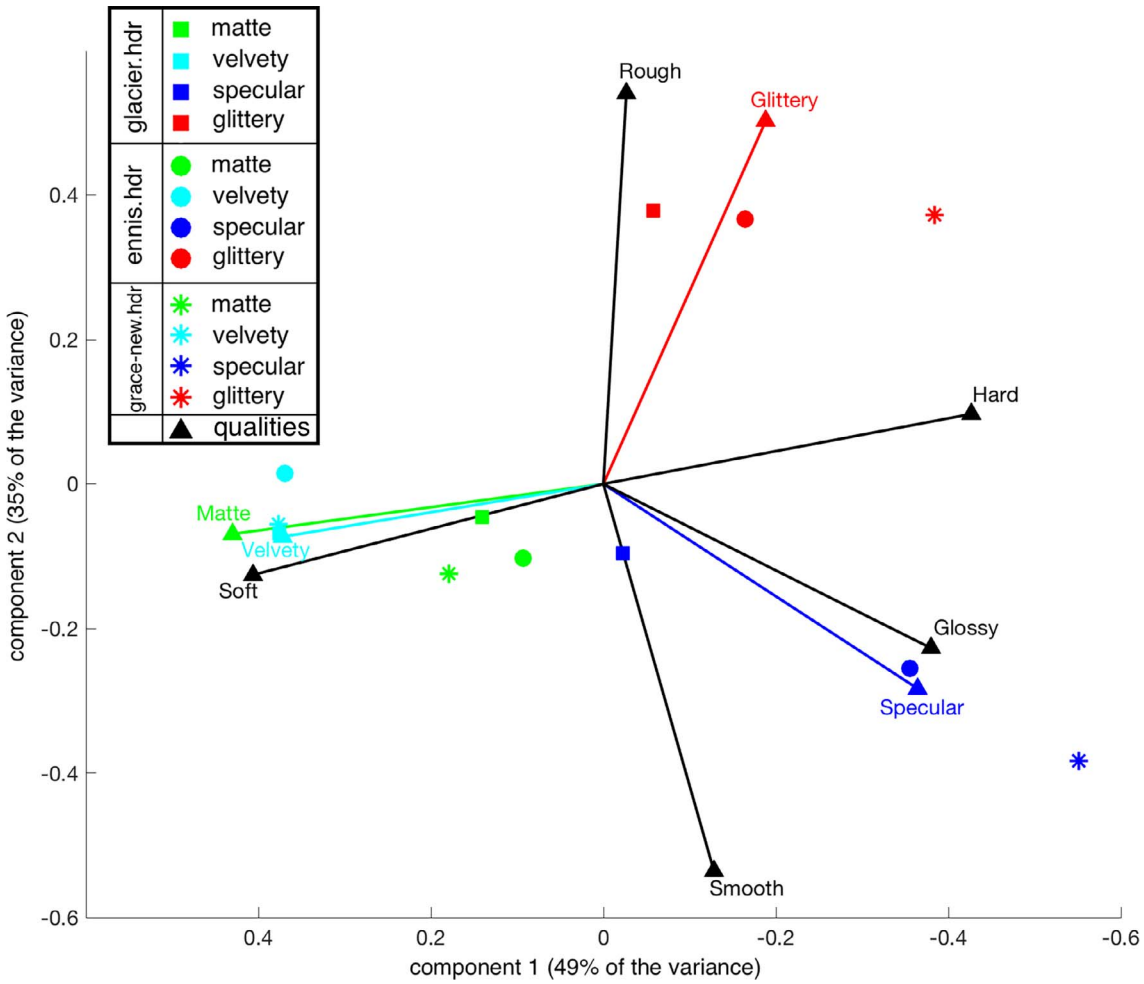

Figure 11. Results of the PCA for Experiment 2. The PCA was done on of the ratings per material quality per stimulus, with the medians determined across all observers and repetitions. The first component (*x*-axis) explains 49% of the variance. The second component (*y*-axis) explains 35% of the variance. The stimuli of the same material mode and corresponding qualities are colored the same, specifically matte in green, velvety in light blue, specular in indigo, and glittery in red. The other five qualities are colored black. The same shape marks the stimuli of the same lighting mode, specifically the Glacier light map as squares, the Ennis light map as circles, and the Grace-new light map as stars.

between the medians of the rating results of Experiment 1 (blue plots) and Experiment 2 (red plots) per material (in the columns), per quality term (in the rows), and as a function of type of lighting. In each subplot, L1 denotes the ambient lighting or the Glacier environment, L2 denotes the focus lighting or the Ennis environment, and L3 denotes the brilliance lighting or the Grace-new environment. With the exception of the matte naming of velvety material, the top four rows of the plots in Figure 12 demonstrate how uniquely the material modes have been associated with their corresponding names, again confirming our previous findings. The bottom five rows of the plots show how the material modes have been associated with the other qualities, acknowledging both hard/soft and rough/smooth as mutually excluding qualities. We found that the overall results from the two experiments correlate highly (the correlation coefficient of all medians of the ratings per material and quality: $r = 0.87, p < 0.001$), suggesting that the selected generic natural lighting environments (blue plots) had similar effects depending on the material mode and quality as the canonical lighting modes (red plots), as was predicted on the basis of the spherical harmonics calculations. A detailed analysis of the impact of the type of lighting on the quality ratings is provided below in the section on material-dependent lighting effects.

We also compared the two PCA spaces (Figures 8 and 11) by rotating the PCA space of Experiment 2 to match that of Experiment 1 on the basis of the coordinates of the nine qualities. Without translation and scaling, the rotating process can be expressed as:

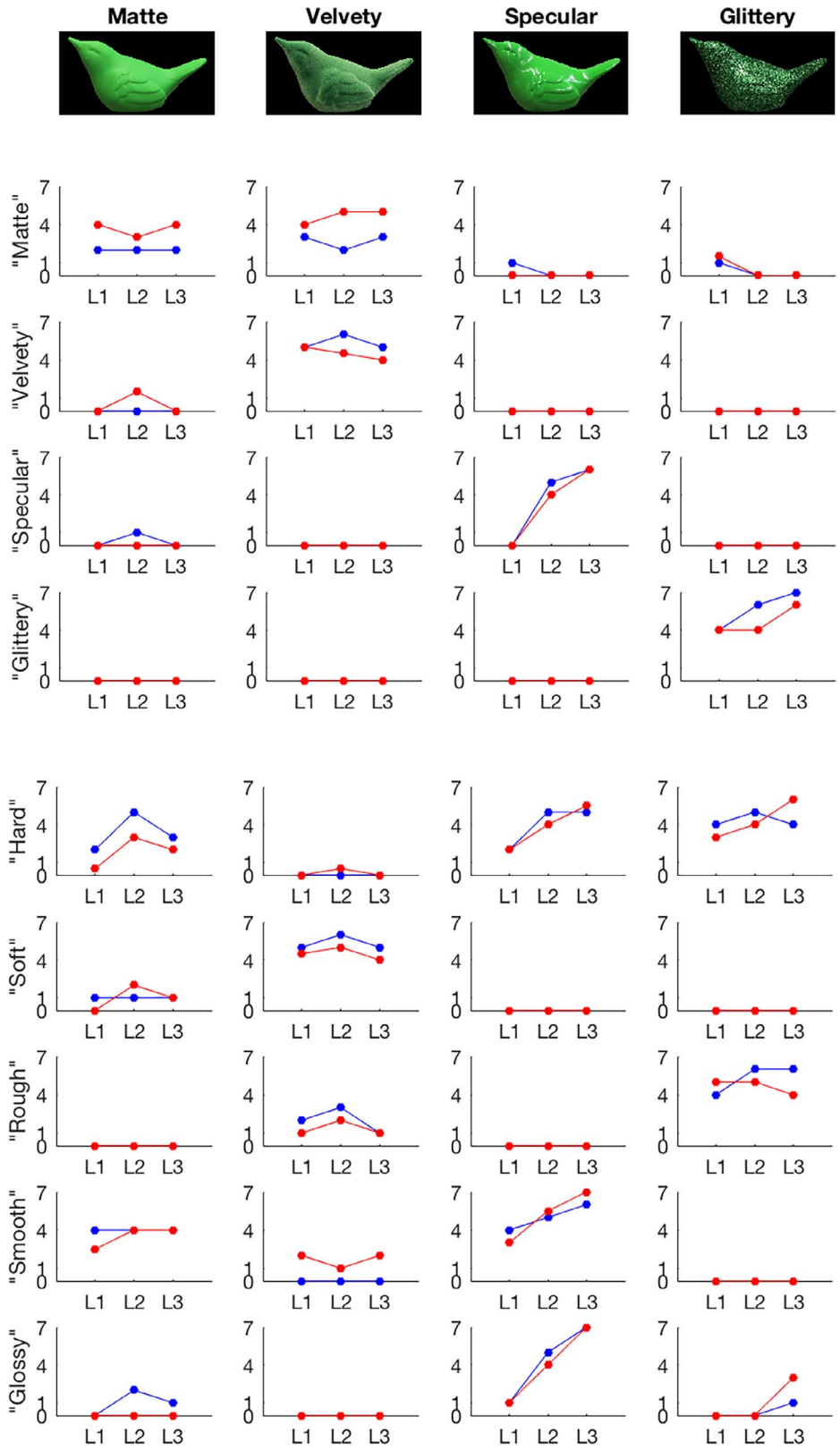

Figure 12. The medians of the ratings per material (columns) and quality term (rows), as a function of lighting. Blue plots are results from Experiment 1 (real stimuli); red plots are results from Experiment 2 (rendered stimuli). In each subplot, L1 denotes ambient lighting or the Glacier environment, L2 denotes focus lighting or the Ennis environment, and L3 denotes brilliance lighting or the Grace-new environment.

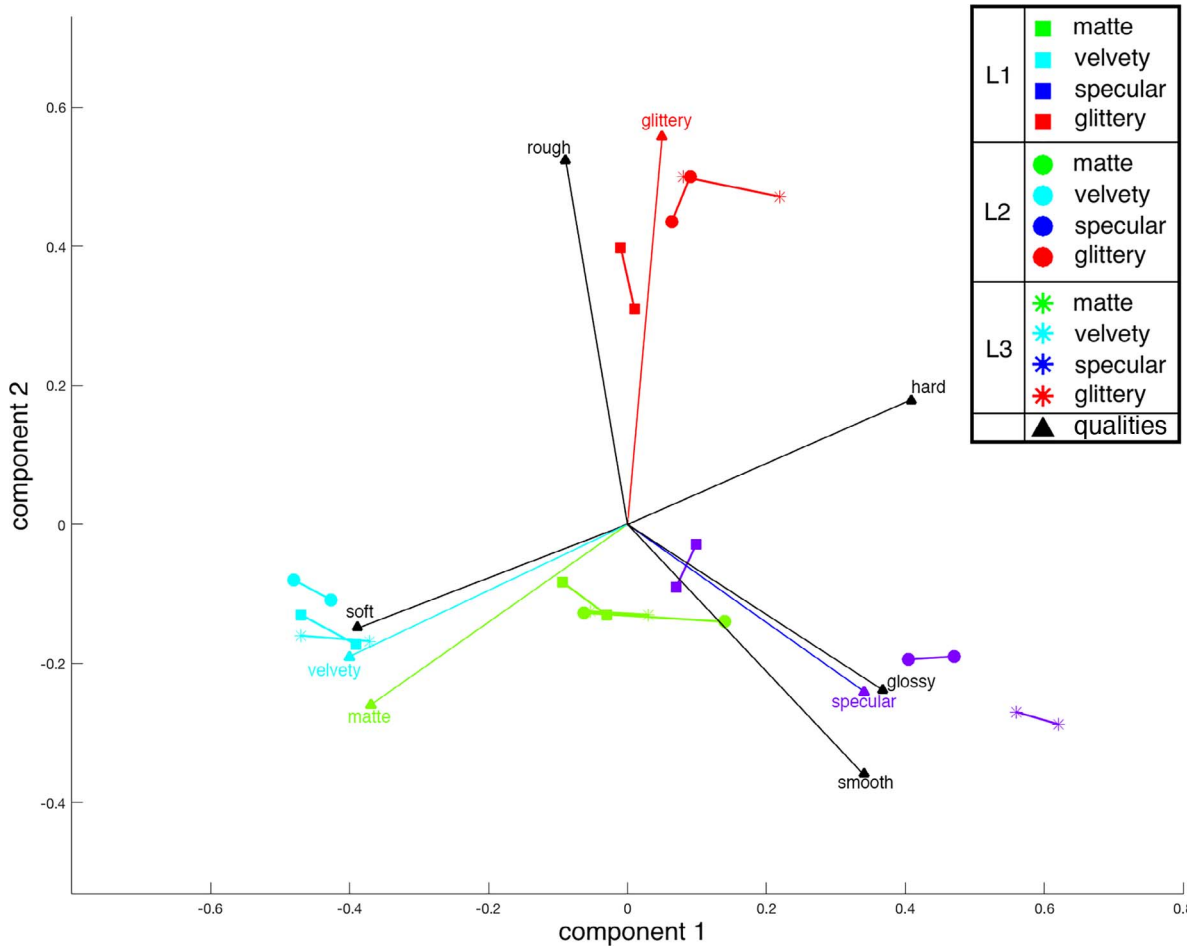

Figure 13. Matching the PCA space of Experiment 2 to that of Experiment 1. The four materials and corresponding qualities are colored in the same format as Figures 8 and 11, specifically matte in green, velvety in light blue, specular in indigo, and glittery in red. The other five qualities are colored black. The same shape marks the stimuli of the same lighting mode, specifically ambient lighting or the Glacier light map as squares (L1), focus lighting or the Ennis light map as circles (L2), and brilliance lighting or the Grace-new light map as stars (L3). The nine qualities from Experiment 1 were marked as triangles. The coordinates of the nine qualities from Experiment 2 overlapped with the corresponding ones from Experiment 1 and thus are not shown for clarity. The data points from the two experiments having the same material (same shape) and lighting mode (same color), have been connected by lines for comparison.

$$[PCA1] = \begin{pmatrix} \cos\theta & \sin\theta \\ -\sin\theta & \cos\theta \end{pmatrix} [PCA2] \quad (8)$$

where $PCA1$ and $PCA2$ both are 2×9 matrices containing the coordinates of the nine qualities in the two spaces, and θ is the angle over which we rotate to match the two spaces. Using least squares minimization, we got a small angle $\theta \approx 13^{\circ}$ with residuals less than 0.09 (negligible). Figure 13 denotes the outcome of the 13° anticlockwise rotation. The data points from the two experiments having the same material (same shape) and lighting mode (same color), have been connected by lines for comparison. The small shifts between these corresponding data points confirm and visualize the high correlation between the results of the two experiments. Note that the coordinates of the nine qualities from Experiment 2 overlapped so much with those from Experiment 1 that they are not included for clarity reasons.

Material-dependent lighting effects

A closer look at Figures 12 and 13 suggests that (a) for matte and velvety materials, some qualities were evoked the most by L2 (i.e., the first order of the SH component) and (b) for specular and glittery materials, some qualities were evoked the most by L3 (i.e., the higher order SH components). To quantitatively validate these possible material-dependent lighting effects, we tested each lighting–material combination for statistical significance by means of two-way ANOVAs, the independent variables *experiment* (two levels) and *lighting* (three levels) being the between-

Material mode	Evoked qualities	Lighting effects
Matte	matte	Evoked by all lightings, independent of experiment: $F_E(1,25)=1.17, p=0.29$, type of lighting: $F_L(2,50)=0.71, p=0.50$, and no interaction effect: $F_I(2,50)=0.86, p=0.43$.
	hard	Evoked the most by L2, somewhat less by L3 and L1: $F_L(2,50)=6.10, p=0.004^{**}$; independent of experiment: $F_E(1,25)=2.03, p=0.17$, and no interaction effect: $F_I(2,50)=0.49, p=0.49$.
	smooth	Evoked by all lightings, somewhat less by L1: $F_L(2,50)=9.49, p<0.001$; independent of experiment: $F_E(1,25)=0.24, p=0.63$and no interaction effect: $F_I(2,50)=2.42, p=0.10$.
Velvety	matte	Evoked by all lightings, somewhat less by L2 in Experiment 1 (interaction effect): $F_I(2,50)=3.88, p=0.03^{*}$; independent of experiment: $F_E(1,25)=2.33, p=0.14$ and type of lighting: $F_L(2,50)=1.17, p=0.32$.
	velvety	Evoked by all lightings, independent of experiment: $F_E(1,25)=0.003, p=0.96$, type of lighting: $F_L(2,50)=1.28, p=0.29$, and no interaction effect: $F_I(2,50)=1.46, p=0.24$.
	soft	Evoked the most by L2, somewhat less by L1 and L3: $F_L(2,50)=6.39, p=0.003^{**}$; independent of experiment: $F_E(1,25)=0.22, p=0.64$and no interaction effect: $F_I(2,50)=1.62, p=0.21$.
	rough	Evoked the most by L2, somewhat by L1 and L3: $F_L(2,50)=14.57, p<0.001$; independent of experiment: $F_E(1,25)=0.29, p=0.60$and no interaction effect: $F_I(2,50)=0.98, p=0.38$.
Specular	specular	Evoked the most by L3, somewhat by L2, the least by L1: $F_L(2,50)=59.94, p<0.001$; independent of experiment: $F_E(1,25)=0.72, p=0.41$and no interaction effect: $F_I(2,50)=1.91, p=0.16$.
	hard	Evoked the most by L3 and L2, somewhat by L1: $F_L(2,50)=8.94, p<0.001$; independent of experiment: $F_E(1,25)=0.00, p=0.99$and no interaction effect: $F_I(2,50)=0.85, p=0.43$.
	smooth	Evoked the most by L3, somewhat by L2, the least by L1: $F_L(2,50)=28.69, p<0.001$;independent of experiment: $F_E(1,25)=0.01, p=0.92$and no interaction effect: $F_I(2,50)=2.93, p=0.06$.
	glossy	Evoked the most by L3, somewhat by L2, not by L1: $F_L(2,50)=77.86, p<0.001$;independent of experiment: $F_E(1,25)=0.47, p=0.50$and no interaction effect: $F_I(2,50)=0.78, p=0.46$.
Glittery	glittery	Evoked the most by L2, somewhat less by L1 and L3 in Experiment 1, the most by L3, somewhat less by L2 and the least by L1 in Experiment 2; main effect of lighting: $F_L(2,50)=59.94, p<0.001$; interaction effect: $F_I(2,50)=9.58p<0.001$; independent of experiment: $F_E(1,25)=4.18, p=0.052$.
	hard	Evoked the most by L2, somewhat less by L1 and L3 in Experiment 1, evoked the most by L3, somewhat less by L2, and the least by L1 in Experiment 2; main effect of lighting: $F_L(2,50)=9.76, p<0.001$;interaction effect: $F_I(2,50)=6.24$, p $=0.004^{**}$; independent of Experiment: $F_E(1,25)=0.004, p=0.95$.
	rough	Evoked by all lightings but the least by L1 in Experiment 1, evoked by all lightings but the least by L3 in Experiment 2; main effect of lighting: $F_L(2,50)=3.36, p=0.04^{*}$, interaction effect: $F_I(2,50)=3.19, p=0.05^{*}$; independent of Experiment: $F_E(1,25)=1.85, p=0.19$.
	glossy	Evoked by L3 only, the most in in Experiment 2; main effect of lighting: $F_L(2,50)=28.95, p<0.001$; interaction effect: $F_I(2,50)=6.66, p=0.003^{**}$; independent of experiment: $F_E(1,25)=0.01, p=0.93$.

Table 3. Summary of the material-dependent lighting effects. L1 denotes ambient lighting or the Glacier environment, L2 denotes focus lighting or the Ennis environment, L3 denotes brilliance lighting or the Grace-new environment. If a quality is not listed for a specific material mode, it was not evoked by any lighting for that material mode. Significance level: $^{*}p < 0.05$, $^{**}p < 0.01$.

subjects and within-subject variable, respectively. The relevant *F*-values can be found in Table 3. Overall, the statistics showed no main effect of the type of experiment; that is, no significant differences between real stimuli (Experiment 1) and rendered ones (Experiment 2), nor substantial interactions between type of experiment and type of lighting. However, there were significant material-dependent effects of the type of

lighting on the qualities. These have been summarized in Table 3. The main findings are: (a) for specular materials, L3 highlights the qualities specular, hard, smooth, and glossy, while L1 reduces these qualities; (b) for glittery materials, L3 highlights and L1 reduces the quality glittery, and to a lesser extent the qualities hard, rough, and glossy; (c) for matte materials, the quality matte is evoked by all lightings, while L2 highlights the quality hard the most; and (d) for velvety materials, the qualities velvety and matte are evoked by all lightings, while L2 highlights to some degree the qualities soft and rough.

General discussion

The Y/N results of both Experiments 1 and 2 have permitted us to assess whether four of the terms we used for material qualities (matte, specular, glittery, and velvety) perceptually correspond to material modes of the same name. From Experiment 1 using real stimuli, we found that the names velvety, specular, and glittery applied to their corresponding material modes, while the name matte applied not only to the matte mode but also to specular and glittery mode under ambient lighting, and to velvety mode under all illuminations. In addition, focus lighting made the matte material look specular (Figure S1). This is in line with our previous work, where we also observed these interactions between matte, velvety, and specular modes and the canonical illuminations (Zhang et al., 2015, 2016), using the same bird object.

One could argue that the association of matte with other material modes in the present study may be due to our matte material mode not representing a perfect diffuse (i.e., Lambertian) material. However, in Experiment 2, we implemented a computer-rendered matte mode using Lambertian material, and found similar results where the name matte also applied to other materials. This suggests that observers confound materials under certain illuminations, as was shown before (Pont & te Pas, 2006; Zhang, de Ridder, & Pont, 2018). An alternative interpretation would be that the semantic meaning of matte is not unique to purely diffusely scattering materials; in particular, velvety was often judged to be a matte material in both experiments, and even more matte than the matte materials, confirming earlier findings (Zhang et al., 2016). Thus, it is not clear what matte means in terms of perception. In terms of optics it can be defined as the diffuse scattering component of a material's reflectance, which is actually present in most materials, and often determines their body color. In a weighted linear superposition model of glossy materials (as often used in computer renderings) matte and glossy form the opposites of the range. In future studies, it might be necessary to investigate whether matte can semantically be considered the opposite of glossy or specular, and define the names of the canonical material modes properly.

One may wonder to which extent the four material modes used in this paper are representative of the space of all possible materials. In Figure 14, we superimposed our results with the 10 material classes from the results of Fleming et al. (2013) obtained from a large number of images from MIT-Flickr database (Sharan, Rosenholtz, & Adelson, 2009) as stimuli. Merging the two sets of results was done by mapping their respective main dimensions: soft–hard and rough–smooth. We note that, on the one hand, each canonical mode represents various classes; on the other hand, the appearance of materials within each class can also vary across canonical modes. Even though our four modes cover the space of materials rather well, there remain material classes that are not covered. For example, if we focus on solid opaque materials, the most notable missing class of materials is metal. Depending on their microstructure, metals may appear to be either smooth and specular, or rough and glittery. Todd and Norman (2018) tested how ambient light influences the perception of metals and found that a combination of ambient and focus lighting was optimal for depicting metals in their experiments. Additional experiments may be required to evaluate the influences of generic illuminations containing higher frequency components, for instance, testing to what extent the brilliance lighting mode influences the perception of metals. Moreover, color effects should certainly be taken into account in such experiments, since those might be diagnostic for the difference between dielectrics and metals (simply said, in dielectrics such as plastics, the highlights have the color of the illumination, while in metal they have the color of the metal).

The rating results from Experiment 1 (real stimuli) and Experiment 2 (rendered stimuli) were strongly correlated, showing that the effects of canonical lightings on material perception are reproducible using generic lighting environments having similar spherical harmonic compositions (i.e., the relative power of SH components). In Figure 3, we could make an interesting observation that, as the scores of the diffuseness metric descended, the scores of the brilliance metric showed a tendency to ascend. This might indicate that SH compositions of generic natural lighting environments may follow these statistical regularities. Another example of such a regularity was found by Mury, Pont, and Koenderink (2009), namely that the positive component of the second order SH component (the so-called *squash tensor*) often aligns with the direction of

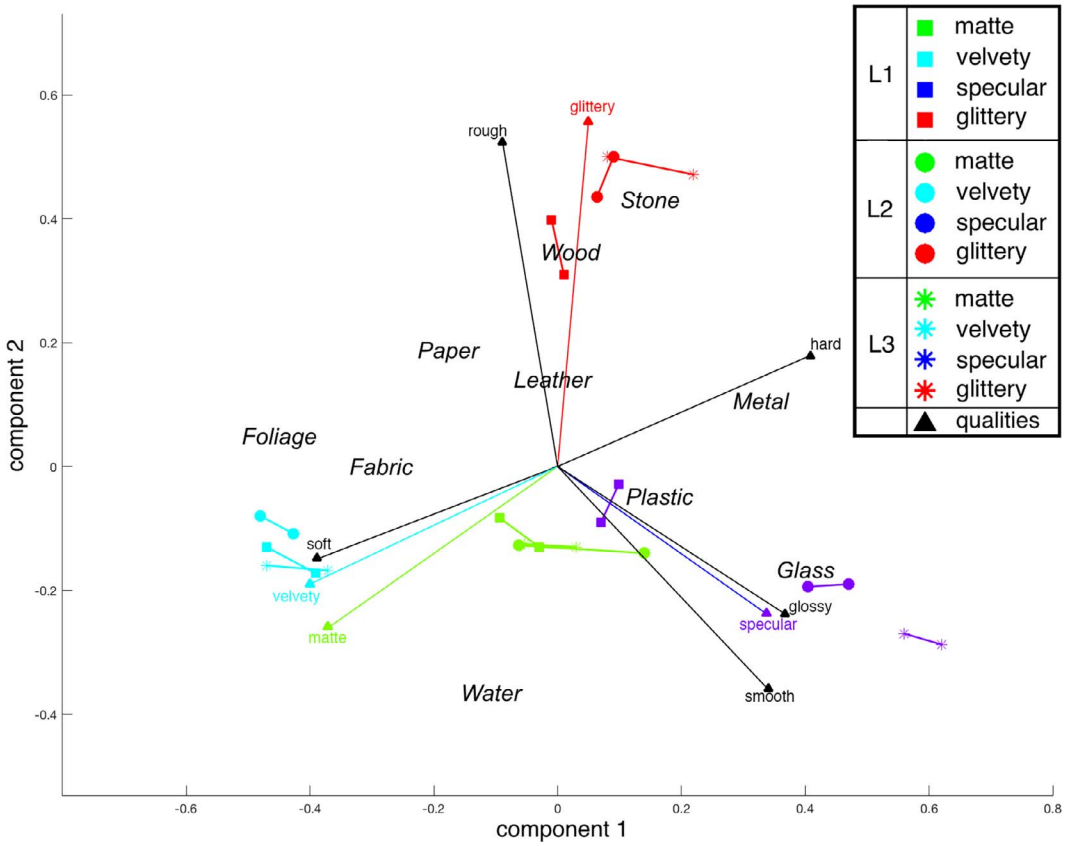

Figure 14. The 10 material classes from previous studies (Sharan et al., 2009; Fleming et al., 2013) mapped onto our PCA space taken from Figure 13.

the first order SH component (the *light vector*) of the light field. This effect is due to reflections from the lighted surface, causing a *light clamp* (Mury et al., 2009). In lighting design, the light clamp does not form a standard component, probably because one gets this effect for free, due to such reflections, and therefore we did not include the squash tensor in our canonical lighting modes and also neglected it in our brilliance metric (Equation 4). The optical cause of the regularity found in the present study might be that the more diffuse the light becomes, the more diffusely scattering the environment has to be, with extreme cases such as a white photo tent or integrating sphere.

Overall, the lighting effects are stronger if the BRDF of the material is more peaked, such as our specular and glittery materials, or general material classes such as metal, plastic, and glass (and even stone, wood, or leather if polished). Corresponding material qualities were evoked the most by lightings that were dominated by higher order SH components, then somewhat less by lightings that were dominated by first order SH component, and the least by lightings that were dominated by a zero-order SH component. On the contrary, if the BRDF is less peaked, the lighting effects are subtler, such as our velvety and matte materials, or fabric, foliage, and paper. Meanwhile, some qualities that associated with matte and velvety materials were evoked the most by lightings that were dominated by a first-order SH component (see Figure 12 and Table 3). The relation between peakedness of the optical functions and the magnitude of the effects might have been expected, since more peaked functions cause larger variations between conditions. The effects for specular and glittery materials might be explained by the observation that the most articulated lighting (brilliance) brings out material properties of materials with peaked BRDFs most, because that combination would lead to the most salient and numerous highlights/glints, being expressions of the most characteristic optic properties of such peaked reflectance. The most bipolar lighting (focus) might be explained to best bring out the characteristic gradients of smoothly varying BRDFs (ambient and brilliance will diffuse out and cause no or fewer strong gradients).

For the specular stimuli in the study of Motoyoshi and Matoba (2012), perceived glossiness changed when varying the contrast and gamma of the illumination. This could be explained in terms of a spherical harmonics decomposition of the illumination. We have applied their contrast and gamma changes to the lighting map they used, Rendering

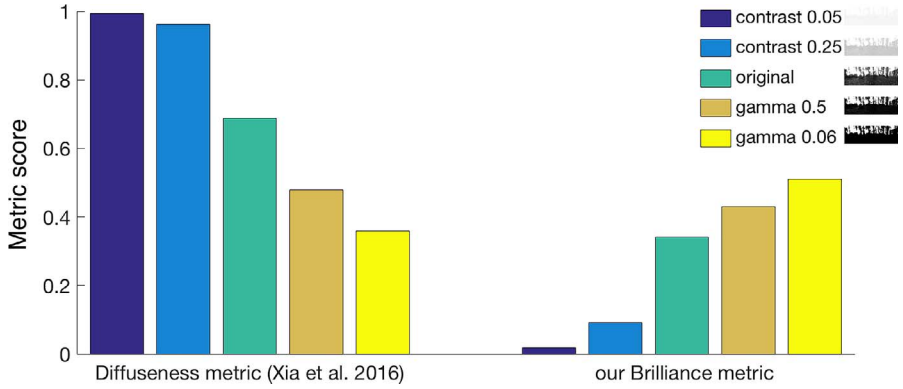

Figure 15. The spherical harmonics–based diffuseness and brilliance analysis for the light maps to which a gamma/contrast change was applied. The original light map was used in the study of Motoyoshi and Matoba (2012). The thumbnails of the light maps are shown next to the legend. The scores of the two metrics negatively correlated ($r = -0.99$, $p < 0.01$).

with Natural Light–eucalyptus (RNL-eucalyptus), and recomputed the SH-based diffuseness and brilliance metrics, as shown in Figure 15. Interestingly, and in line with what can be seen in Figure 3, we found that the scores of the diffuseness metric descended as the scores of the brilliance metric ascend ($r = -0.99$, $p < 0.01$). Here, a lowering of the contrast in the lighting could be interpreted as an increase of the zero-order SH component and a decrease of higher-order SH components, which tends to make the specular surface look more matte. A lowering of the gamma in the lighting could be interpreted as an increase of higher-order SH components and decrease of the zero-order SH component, and thus could evoke the perception of the glossy quality for specular surfaces. One notable advantage of SH-based metrics is that it provides absolute values that permit comparisons between different environments. In future work, it would be interesting to study how manipulating the relative power of SH components could affect material perception in a controllable way, with potential applications in the field of computer graphics. One possibility would be to express both material and lighting in terms of SH coefficients (as done by Ramamoorthi & Hanrahan, 2001, for inverse rendering). However, spherical harmonics characterize a lighting environment in a global fashion: for instance, simply rotating the lighting with respect to the object has the potential to affect material perception but leaves the spherical harmonic coefficients unchanged. This perceptual effect is shown in Figure 16, where the perceived material of the specular bird seems to change significantly when it is rotated in the focus canonical lighting. This holds for various materials, as was shown using computer graphics methods (e.g., Bousseau, Chapoulie, Ramamoorthi, & Agrawala, 2011) and conforms with the practice of optimizing the orientation of lighting to maximize heuristic measurements inspired from photographic practices (Hunter et al., 2015). More metrics are needed for detailed analysis of illuminations beyond the first order SH, to quantify their spatial structures (the type of light texture (e.g., dotted or stripy studio lighting). In a subsequent work, we will study how the orientation of a lighting environment or the shape of the object may affect material appearance depending on the choice of material mode.

Conclusion

We investigated (a) how canonical material modes associate with perceived material qualities and (b) how canonical lighting modes brought out the perception of material qualities for each material. In combination with four canonical material modes (matte, velvety, specular, and glittery) and three canonical lighting modes (ambient, focus, and brilliance), 12 stimuli were rated for nine material qualities, namely matte, velvety, specular, glittery, glossy, rough, smooth, hard, and soft. Material-dependent lighting effects were found. Specifically, we performed a pair of experiments in which we presented observers with images of an object made of four materials in three lightings, and asked them to rate each configuration according to nine material qualities. In the first experiment, the stimuli were photographs of real objects lit by canonical lightings, while in the second experiment, the stimuli were rendered using state-of-the-art surface reflectance models for the four material modes lit by three environment maps as illuminations. Three environment maps were selected to represent our canonical lighting modes based on a diffuseness metric and a brilliance metric (Figure 3), namely the Glacier, Ennis, and Grace-new environments for the ambient, focus, and brilliance light, respectively. We made

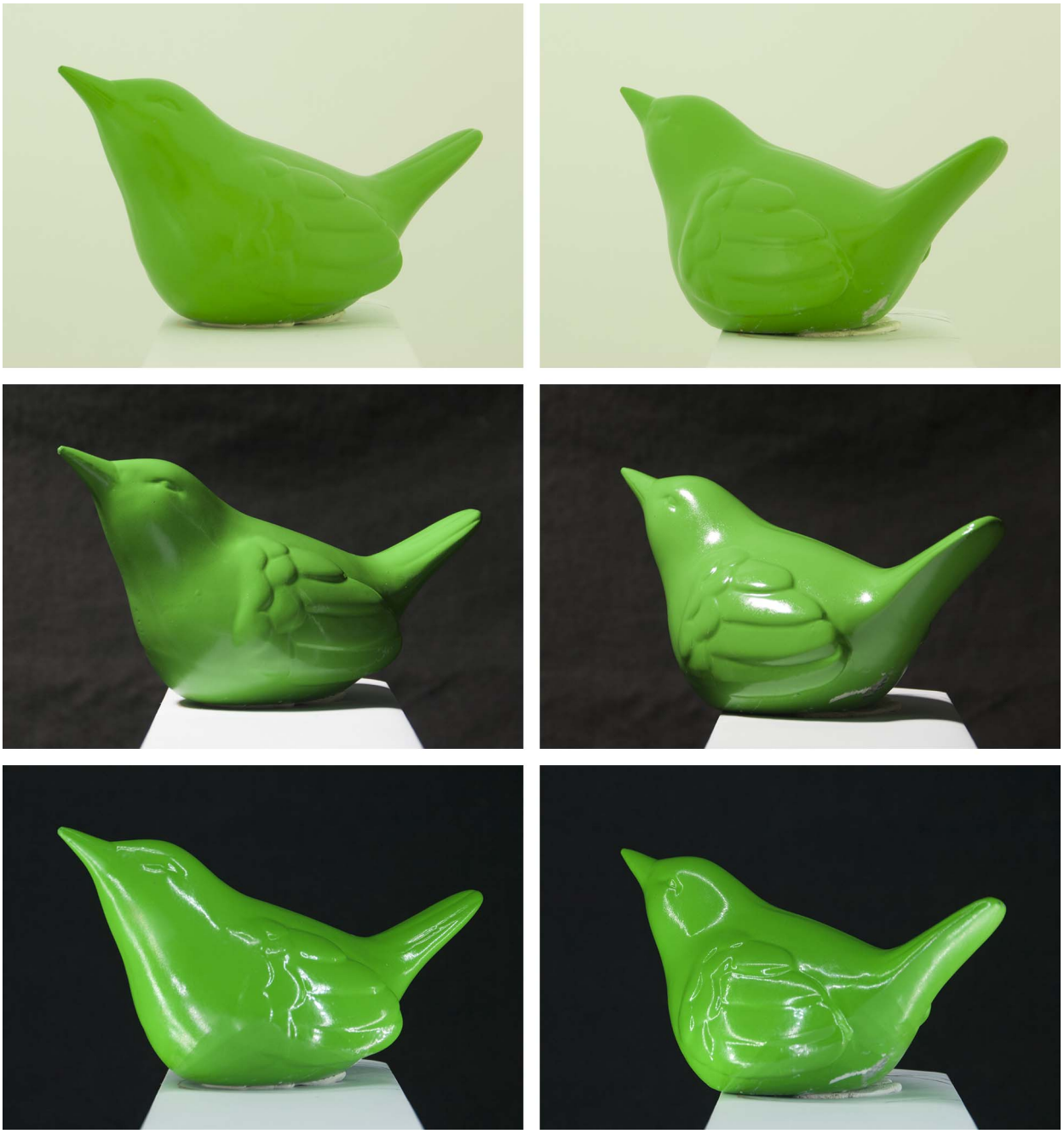

Figure 16. With a fixed viewing angle, either rotating the illumination or the illuminated object may result in changes in appearance and thus give a different perception. From top to bottom, each row shows the same specular object in two orientations under ambient, focus, and brilliance light, respectively. Its appearance varies the most across the two orientations when using focus lighting (second row).

predictions of the effects of lighting on material appearance for generic natural lighting environments and validated the predictions: results correlated strongly for the two experiments and reproduced material-dependent lighting effects of former studies. Our results support the notion that systematically varying the spatial structure of the natural illumination, such as enhancing or attenuating the corresponding modal components of the lighting, can systematically evoke the perception of associated material qualities. The optics-based models span a wide range of natural materials and lighting environments, providing a systematic approach to study the perceptual interactions of materials and lighting.

Keywords: photography, *lighting effects*, *material perception*, *canonical modes*, *natural lighting environments*

Acknowledgment

This work has been funded by the EU FP7 Marie Curie Initial Training Networks (ITN) project PRISM, Perceptual Representation of Illumination, Shape and Material (PITN-GA-2012-316746). Special thanks to Dr. Rene van Egmond for the helpful discussions.

Commercial relationships: none.
Corresponding author: Fan Zhang.
Email: f.zhang-2@tudelft.nl.
Address: Perceptual Intelligence Lab, Faculty of Industrial Design Engineering, Delft University of Technology, Delft, The Netherlands.

References

Barati, B., Karana, E., Sekulovski, D., & Pont, S. C. (2017). Retail lighting and textiles: Designing a lighting probe set. *Lighting Research & Technology*, *49*(2), 173–194.

Bousseau, A., Chapoulie, E., Ramamoorthi, R., & Agrawala, M. (2011). Optimizing environment maps for material depiction. *Computer Graphics Forum*, *30*(4), 1171–1180.

Brainard, D. H. (1997). The psychophysics toolbox. *Spatial Vision*, *10*, 433–436.

Debevec P. E. (1998). Rendering synthetic objects into real scenes: Bridging traditional and image-based graphics with global illumination and high dynamic range photography. In *Proceedings of SIGGRAPH 98. Computer Graphics Proceedings. Annual Conference Series* (pp. 189–198). New York, NY: ACM Press.

Döerschner, K., Boyaci, H., & Maloney, L. T. (2010). Estimating the glossiness transfer function induced by illumination change and testing its transitivity. *Journal of Vision*, *10*(4):8, 1–9, https://doi.org/10.1167/10.4.8. [PubMed] [Article]

Dror, R. O., Willsky, A. S., & Adelson, E. H. (2004). Statistical characterization of real-world illumination. *Journal of Vision*, *4*(9):11, 821–837, https://doi.org/10.1167/4.9.11. [PubMed] [Article]

Fleming, R. W., Dror, R. O., & Adelson, E. H. (2003). Real-world illumination and the perception of surface reflectance properties. *Journal of Vision* *3*(5):3, 347–368, https://doi.org/10.1167/3.5.3. [PubMed] [Article]

Fleming, R. W., Wiebel, C., & Gegenfurtner, K. (2013). Perceptual qualities and material classes. *Journal of Vision*, *13*(8):9, 1–20, https://doi.org/10.1167/13.8.9. [PubMed] [Article]

Ganslandt, R., & Hofmann, H. (1992). *Handbook of interior lighting*. Lüdenscheid, Germany: ERCO.

Hunter, F., Biver, S., & Fuqua, P. (2015). Light science & magic: An introduction to photographic lighting. Boca Raton, FL: CRC Press.

Kelly, R. (1952). Lighting as an integral part of architecture. *College Art Journal*, *12*(1), 24–30.

Kleiner, M., Brainard, D., Pelli, D., Ingling, A., Murray, R., & Broussard, C. (2007). What's new in Psychtoolbox-3. *Perception*, *36*(14), 1–16.

Koenderink, J., & Pont, S. (2003). The secret of velvety skin. *Machine Vision and Applications*, *14*(4), 260–268.

Lagae, A., & Drettakis, G. (2011, August). Filtering solid Gabor noise. In *ACM Transactions on Graphics (TOG)*, (Vol. 30, No. 4, p. 51). New York, NY: ACM.

Lagae, A., Lefebvre, S., Drettakis, G., & Dutré, P. (2009, July). Procedural noise using sparse Gabor convolution. In *ACM Transactions on Graphics (TOG)*, (Vol. 28, No. 3, p. 54). New York, NY: ACM.

Marlow, P., Kim, J., & Anderson, B. L. (2011). The role of brightness and orientation congruence in the perception of surface gloss. *Journal of Vision*, *11*(9):16, 1–12, https://doi.org/10.1167/11.9.16. [PubMed] [Article]

Marlow, P., Kim, J., & Anderson, B. L. (2012). The perception and misperception of specular surface reflectance. *Current Biology*, *22*(20), 1909–1913.

Motoyoshi, I., & Matoba, H. (2012). Variability in constancy of the perceived surface reflectance across different illumination statistics. *Vision Research*, *53*(1), 30–39.

Mury, A. A., Pont, S. C., & Koenderink, J. J. (2007). Light field constancy within natural scenes. *Applied Optics*, *46*(29), 7308–7316.

Mury, A. A., Pont, S. C., & Koenderink, J. J. (2009). Structure of light fields in natural scenes. *Applied Optics*, *48*(28), 5386–5395.

Olkkonen, M., & Brainard, D. H. (2010). Perceived glossiness and lightness under real-world illumination. *Journal of Vision*, *10*(9):5, 1–19, https://doi.org/10.1167/10.9.5. [PubMed] [Article]

Pont, S. C. (2009, February). Ecological optics of natural materials and light fields. In *Human Vision and Electronic Imaging XIV* (*Vol. 7240*, p. 724009). Bellingham, WA: International Society for Optics and Photonics. https://doi.org/10.1117/12.817162.

Pont, S. C., & te Pas, S. F. (2006). Material-

illumination ambiguities and the perception of solid objects. *Perception*, *35*(10), 1331–1350.

Ramamoorthi, R., & Hanrahan, P. (2001). A signal-processing framework for inverse rendering. In *Proceedings of the 28th Annual Conference on Computer Graphics and Interactive Techniques (SIGGRAPH '01)*. New York, NY: ACM Press/Addison-Wesley Publishing Co.

Sharan, L., Rosenholtz, R., & Adelson, E. (2009). Material perception: What can you see in a brief glance? [Abstract]. *Journal of Vision*, *9*(8): 784, https://doi.org/10.1167/9.8.784. [Abstract]

Stock, R. D., & Siegel, M. (1996). Orientation invariant light source parameters. *Optical Engineering*, *35*(9), 2651–2661.

Stokes, M., Anderson, M., Chandrasekar, S., & Motta, R. (2012). *A standard default color space for the Internet—sRGB, 1996*. http://www.w3.org/Graphics/Color/sRGB.

Todd, J. T., & Norman, J. F. (2018). The visual perception of metal. *Journal of Vision*, *18*(3):9, 1–17, https://doi.org/10.1167/18.3.9. [PubMed] [Article]

van Assen, J. J. R., Wijntjes, M. W., & Pont, S. C. (2016). Highlight shapes and perception of gloss for real and photographed objects. *Journal of Vision*, *16*(6):6, 1–14, https://doi.org/10.1167/16.6.6. [PubMed] [Article]

Vergne, R., & Barla, P. (2015). Designing Gratin, a GPU-tailored node-based system. *Journal of Computer Graphics Techniques*, *4*(4), 54–71.

Ward, G. J. (1992). Measuring and modeling anisotropic reflection. *ACM SIGGRAPH Computer Graphics*, *26*(2), 265–272.

Xia, L., Pont, S. C., & Heynderickx, I. (2017). Light diffuseness metric part 1: Theory. *Lighting Research & Technology*, *49*(4), 411–427.

Zhang, F., de Ridder, H., Fleming, R. W., & Pont, S. (2016). MatMix 1.0: Using optical mixing to probe visual material perception. *Journal of Vision*, *16*(6):11, 1–18, https://doi.org/10.1167/16.6.11. [PubMed] [Article]

Zhang, F., de Ridder, H., & Pont, S. C. (2015, March). The influence of lighting on visual perception of material qualities. In B. E. Rogowitz, T. N. Pappas, & H. de Ridder (Eds.), *Proceedings of SPIE 9394, Human Vision and Electronic Imaging XX* (p. 93940Q). https://doi.org/10.1117/12.2085021.

Zhang, F., de Ridder, H., & Pont, S. C. (2018). Asymmetric perceptual confounds between canonical lightings and materials. *Journal of Vision*, *18*(11):11, 1–19, https://doi.org/10.1167/18.11.11. [PubMed] [Article]